Plasmon resonances in linear atomic chains: Free-electron behavior and anisotropic screening of *d* electrons

Jun Yan and Shiwu Gao
Institute of Physics, Chinese Academy of Sciences, 100190 Beijing, China
and Department of Physics, Göteborg University, SE-41296 Göteborg, Sweden
(Received 4 October 2008; revised manuscript received 4 November 2008; published 8 December 2008)

Electronic excitations in linear atomic chains of simple and noble metals (silver) have been studied using time-dependent density-functional theory. The formation and development of collective resonances in the absorption spectra were obtained as functions of the chain length. A longitudinal collective resonance appears in both simple- and noble-metal chains. Its dispersion has been deduced and is compared with that of a one-dimensional electron gas. The transverse excitation generally shows a bimodal structure, which can be assigned as the "end and central resonances." The *d* electrons of silver atoms reduce both the energies and intensities of the transverse modes but have little effect on its longitudinal resonance. This anisotropic screening is determined by the interband ($d \rightarrow p$) transition, which is involved only in transverse oscillations. Analysis of these results yields a general picture of plasmon resonances in one-dimensional atomic structures. Implications of such atomic-scale plasmons to surface plasmons in larger dimensions are also discussed.

DOI: 10.1103/PhysRevB.78.235413 PACS number(s): 72.15.Nj, 73.20.Mf, 71.45.Gm

I. INTRODUCTION

During the past few years, surface plasmons in nanostructures[1–24] have attracted much attention in nanosciences. Different from the bulk[25] and surface-plasmon waves,[26–29] nanostructures sustain localized surface-plasmon resonances (LSPRs) on their confining boundaries, leading to dynamic charge accumulation and field enhancement near their surfaces. Such collective oscillations and the decay at surfaces are responsible for the novel applications in optical imaging,[22] single-molecule sensing and spectroscopy,[1,2] photocatalytic reactions,[23] and cancer therapy.[24] As a general feature, the frequencies of LSPRs show sensitive dependences on the sizes, shapes, and surrounding environment. Such dependences are often interpreted classically as geometric effect by classical electrodynamic models.[30,31] In particular, the plasmon hybridization model developed by Nordlander and co-workers[15–21] has been very successful in predicting the energetics of complex structures and providing a transparent physical picture of LSPRs. Most experiments done so far are focused exclusively on structures that are sized between a few-tenth and few-hundred nanometers, where it can be expected that the LSPRs could behave classically.

Contrary to the rapid development in the classical modeling of plasmon energetics, microscopic understanding of LSPRs and its connection to the electronic structures of the systems are still missing. In particular, information about the decay dynamics of surface plasmons, which plays the central role in plasmon-mediated processes, is not available in any classical description. This concern becomes more relevant in reduced dimensions when quantization introduced by confinement becomes more prominent in the one-particle spectra. It is thus far unclear how quantization in the one-particle spectra interplays with and manifests in their collective excitations. These issues have only been studied in a few cases including two-dimensional (2D) thin films[32,33] and spherical nanoparticles,[34–36] where quantum oscillations in plasmon frequencies and lifetime have been observed. In the present study, we take a quantum-mechanical approach to a simple model system, one-dimensional (1D) atomic chains with variable lengths. Our aim was to find out, on a conceptual basis, how collective excitations in atomic dimensions derive from their electronic structures and how these atomic plasmons compare with surface plasmons in the classical regime in terms of energetics and real-time electron dynamics. The answers to these questions are not only interesting for the 1D plasmons of atomic chains but also have implications to the general understanding of LSPRs in the quantum regime.

Experimentally, linear atomic chains have been created and studied both as a model system for fundamental studies and as potential conducting wires for device applications. Supported chains were formed by manipulation of adsorbed atoms on solid surfaces,[37] while suspended chains were also made in break junctions.[38,39] Their structures[40–42] and electronic properties[43–46] have been intensively investigated by various experiments. In particular, Ho and co-workers[47] first demonstrated the formation of one-dimensional band structure out of individual atomic states as the chain length increases atom by atom. Spatial-resolved tunneling spectroscopy identified standing waves along the chains and end states,[48] whose electron densities are localized at the ends of the chains at certain resonance energies. The spectra of the single-particle states could be qualitatively understood by the particle-in-a-box model. Very recently, collective plasmon excitation has been observed in Au wires on a Si(557) surface.[49,50] Its energy dispersion is characteristic for plasmons in one-dimensional electron gas (1DEG). In earlier experiments, plasmon excitation was also speculated to play a role in the light-emission spectroscopy of atomic chains[51] and photoconductance enhancement[52] of atomic-sized tunnel junctions under laser radiation. Yet it is unclear how and which plasmon mode of the complex structures (tip, substrate, or atom chains) was involved in these experiments.

A brief report on the plasmon resonances of sodium chains was given in early publications[53,54] using both

TABLE I. Numerical parameters used in the time propagation. From left to right are the atom species with their electronic configuration, the radius R of the simulation sphere around each atom, the spacing of the grid Δx, the time step Δt, and the total propagation time T.

	Pseudopotentials	R (Å)	Δx (Å)	Δt ($\hbar$/eV)	T ($\hbar$/eV)
Na ($3s^1$)	TM2[a,b]	8	0.5	0.005	50
K ($4s^1$)	HGH[c]	8	0.3	0.005	50
Ag ($5s^1$)	HGH	6	0.3	0.005	50
Ag ($4d^{10}5s^1$)	TM2[a,d]	6	0.25	0.003	50
Ag (theor.)	TM2[e,f]	6[e]	0.25,[e] 0.24[f]	0.001[e]	50[f]

[a]Scalar-relativistic Troullier-Martins pseudopotentials (Ref. 58) in nonlocal form (Ref. 59).
[b]Generated from the $3s^1 3p^0 3d^0 4f^0$ reference configuration with core radii $r_{cs}=r_{cp}=r_{cd}=r_{cf}=2.94$ a.u.
[c]Hartwigsen-Goedecker-Hutter pseudopotentials.
[d]Generated from the $5s^1 5p^0 4d^{10} 4f^0$ reference configuration with core radii $r_{cs}=r_{cp}=r_{cd}=r_{cf}=2.34$ a.u.
[e]Reference 60.
[f]Reference 61.

electron-gas model and atomistic model based on time-dependent density-functional theory (DFT) (TDDFT). Here, we present more detailed and systematic results for several atom chains built with simple metals (Na and K) and noble metal (Ag). Our extensive calculations confirmed the general existence of a longitudinal (L) and two transverse (T) plasmon resonances (TE and TC) in all these chains. The nature and electron dynamics of these modes are elaborated. We found that the d electrons of silver atoms have little effect on the frequency and strength of longitudinal mode but strongly quench the transverse excitation. This anisotropic screening of d electrons is governed by the energetics of interband transitions, which is only operative in transverse excitations. In addition, the excitation spectra with variable interatomic distances are also calculated, shedding light on the physical origin of energy splitting in the transverse excitations. Finally several aspects of the 1D plasmon resonances of atomic chains including energy dispersion and tunability are discussed.

The rest of this paper is organized as follows. The computational methods and numerical parameters are detailed in Sec. II. Section III presents the excitation spectra of various chains. The effect of d electrons on the plasmon resonances in silver is studied in detail. A brief summary is given in Sec. IV.

II. COMPUTATIONAL METHODS

All of our calculations were performed with a real-space and real-time TDDFT code OCTOPUS (Ref. 55) as used in a previous publication.[54] The atoms were described by norm-conserving pseudopotentials, whose parameters were given in Table I. Local-density approximation (LDA) for the exchange-correlation potential was used in both the ground-state and excited-state calculations. The simulation zone was defined by allocating one sphere around each atom. The electronic wave functions were represented on a uniform mesh inside the simulation zone, as detailed in Table I. In the real-time propagation, excitation spectrum was extracted by Fourier transform of the dipole strength[56] induced by an impulse excitation. To double check our results, linear-response (LR) formalism in frequency domain[57] was also calculated for shorter chains. For all systems we compared, the frequency-domain calculations give essentially the same excitation spectra. The time-evolution scheme is however faster for large systems and yields more information on the real-time dynamics of the electrons. The results in this paper are mainly based on time-domain calculations.

All major parameters for the ground-state DFT calculation and time propagation are listed in Table I. Two different norm-conserving pseudopotentials[58,59] were used for silver atoms. The chosen radius and mesh size assure an energy convergence of ground state and excitation spectra within 0.1 eV for all chains. For silver chains, valence electrons are more localized than those in Na and K chains. A smaller atomic radius of 6 Å is enough to reach the same accuracy.[60] Representation of the d-electron wave functions requires, however, finer mesh size.[60,61] The time step Δt is controlled by the mesh size Δx. We found that for an efficient and stable time propagation, optimal values of the time step are $\Delta t = 0.005\ \hbar/\mathrm{eV}$ for Na and K atoms and $0.003\ \hbar/\mathrm{eV}$ for Ag atoms,[60] respectively. For all the chains calculated, the electronic wave packets were evolved by a total time of $T = 50\ \hbar/\mathrm{eV}$, which yields an energy resolution of around 0.02 eV in the excitation spectra.

III. RESULTS AND DISCUSSION

We start with presenting detailed results of Na chains including data of higher-order longitudinal modes. The dependence of transverse excitation on the interatomic distances is also presented and discussed. This is followed by a comparative study of K chains. Common features and differences of their plasmon resonances are discussed. In Sec. III B, we present results of Ag chains using pseudopotentials with and without d electrons, such that the role of d electrons in the low-energy excitations is elaborated. Finally in Sec. III C, we focus on a few general aspects of 1D plasmons including energy dispersion, comparison with classical models, and tunability at atomic scale.

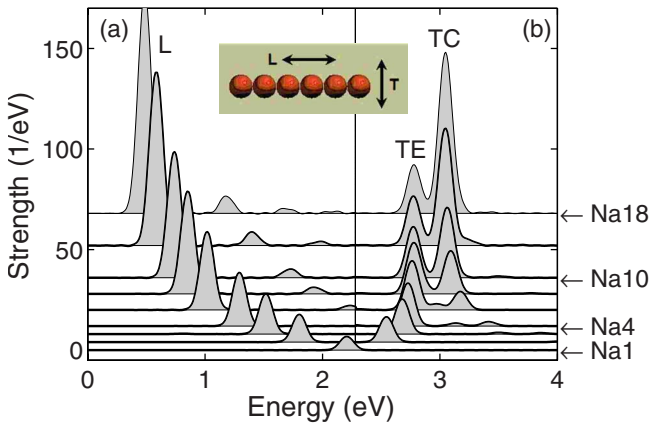

FIG. 1. (Color online) The dipole response (optical absorption) of linear sodium chains, with variable number of atoms N, to an impulse excitation with momentum increase $\delta k = 0.05/\text{Å}$ polarized in the (a) longitudinal and (b) transverse directions. The series of spectra correspond, counting from the bottom, to $N=1$, 2, 3, 4, 6, 8, 10, 14, and 18.

A. Plasmon resonances in simple atom chains: Na and K

Figure 1 shows the dipole strength of the sodium chains as a function of the length under longitudinal (L, left panel) and transverse (T, right panel) excitations. The polarization was simulated by applying an impulse along or perpendicular to the chains, respectively. As discussed in our previous publication,[54] the excitation spectra exhibit one L and two T modes: the end and central modes. The frequencies of these modes are slightly smaller than the data shown in Ref. 54 because a larger interatomic distance $d=3.72$ Å corresponding to the bond length of a free dimer[62] has been used in the present calculation. As the length of the chain increases, the energy of the L mode decreases gradually from 1.52 eV in the three-atom chain Na3 to 0.49 eV in Na18. This redshift results mainly from the reduction in the energy gaps with the increased chain length. Meanwhile, the intensity of the L mode increases linearly as a function of the chain length, demonstrating the accumulation of collectivity in the excitation as more electrons participate in the collective oscillation. Apart from the lowest dipole mode, high-energy modes are also discernible in longer chains, for example, the 1.18 and 1.66 eV modes in Na18 (the topmost curve). As we shall see later, these modes are higher-order excitations ($n=2$ and $n=3$) with multiple nodes in the density response along the chains.

The evolution of the two T modes, panel (b) in Fig. 1, differs substantially from that of the L mode. Figure 2 shows the length dependence of (a) the energies and (b) the oscillator strengths of the two T modes. Both modes gain intensity as the chain length increases. However, for chains shorter than five atoms, the spectra are dominated by the low-energy mode at 2.7 eV, the end mode. From Na5, the high-energy mode (central mode) increases in intensity and develops into a well-defined resonance, which is separated from the end mode by a finite-energy gap. As the length further increases, intensity of the end mode becomes saturated with an integral oscillator strength of about four electrons, while the strength of the central mode grows almost linearly with the length, after it shows up at Na5.

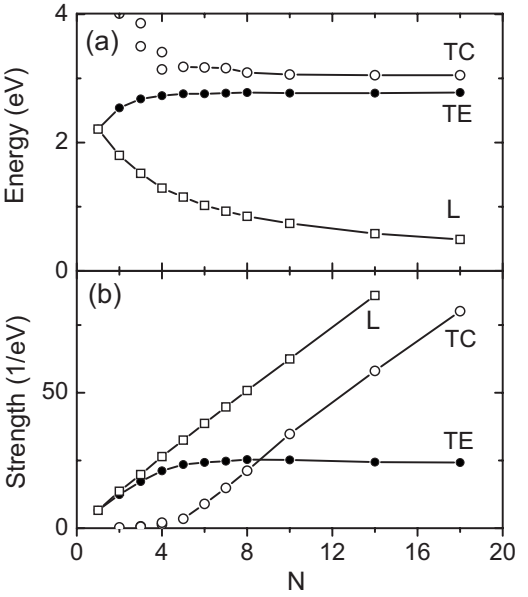

FIG. 2. (a) The excitation energy and (b) the dipole strength as functions of the number of atoms N for the three resonance peaks shown in Fig. 1. They are assigned to the longitudinal (ω_L) and transverse plasmon modes (ω_{TE} and ω_{TC}), as discussed in the text.

The nature of these resonances can be analyzed by the induced charge densities at the resonance frequencies. Figure 3 shows the Fourier transform of the induced densities of the three L modes ($n=1$, 2, and 3, respectively) in the Na18 chain projected in the atomic plane. The density responses of these modes are asymmetric across the chain with maximum at one end and minimum at the other, showing dipole character of the plasmon oscillation. Along the chains, the density envelope is monotonic for the $n=1$ mode but exhibits oscillatory structures for the $n=2$ and 3 modes, with n oscillation periods, resulting from the longitudinal quantization of plasmon in one dimension. In addition, the densities also show rapid variations around the atomic sites modulated by local atomic potentials. These variations are similar in all three L modes, suggesting that they are local modulations by

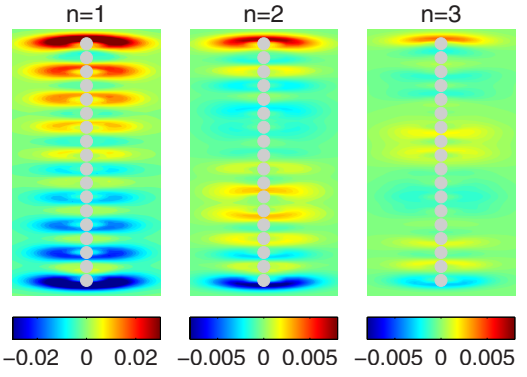

FIG. 3. (Color online) Fourier transforms of the induced densities at, from left to right, plasmon resonances of 0.49, 1.18, and 1.66 eV, respectively, for the Na18 chain shown in Fig. 1. The filled circles indicate the positions of the atoms.

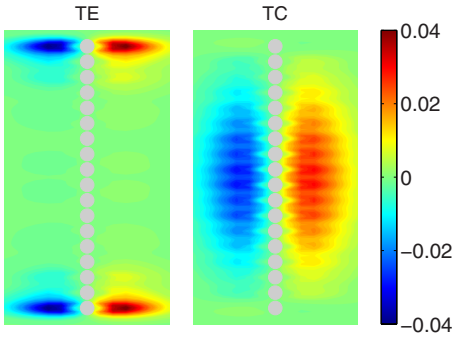

FIG. 4. (Color online) Fourier transforms of the induced densities at the two transverse plasmon resonances ω_{TE} (left) and ω_{TC} (right) for Na18.

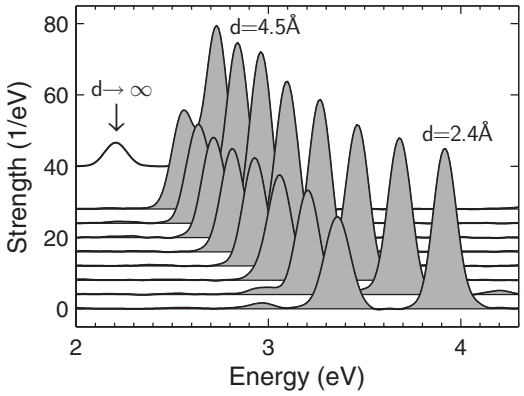

FIG. 5. The optical absorption of Na12 as a function of interatomic distance d. The spectra correspond, from bottom to top, to a series of d varied from 2.4 to 4.5 Å incrementally by 0.3 Å. The arrow marks the dipole resonance energy of a single Na atom.

the intra-atomic potential. The density profiles in Fig. 3 for different states demonstrate the competition between global quantization and local atomic confinement. Quantization effect was also observed in earlier electron-gas model.[53] However, atomic modulation only shows up in the atomistic modeling given in Fig. 3. It will be interesting to find out whether these features are intrinsic to the atomic chains or general to other nanostructures such as nanoparticle arrays.

Figure 4 shows the induced densities of the two transverse modes in Na18 at ω_{TE} (left panel) and ω_{TC} (right panel), which are localized at the two ends and center of the chain, respectively. The spatial distributions of these two modes, as a function of the chain length, had been analyzed in detail in our previous work.[54] They are consistent with the evolution of energies and strengths of the two modes shown in Fig. 2. It is interesting to note that charge distribution of the end mode is localized exclusively on the end atoms, while that of the central mode has nearly vanishing amplitude on the atoms at the ends. Such a spatial separation in the transverse excitation of atomic chains resembles the density response of the surface and bulk plasmons of solid surfaces and thin films. The surface (end) plasmon is lower in energy than the bulk (central) plasmon. Their densities are localized in different regions in space. We expect that such end and central modes also exist in other one-dimensional structures, such as nanowires and nanotubes, which will be under future investigations.

The energy splitting in the transverse excitation may originate from the following differences between the end and central atoms: (i) the position-dependent electron potential, which is highest at the two ends and lower in the center of the chains, and (ii) electron-electron interaction, which differs between the end and central atoms due to the dangling bonds at the ends. Both quantities are dependent on d, the interatomic distance. The splitting should diminish at increasing d and completely disappear in the large d limit, where the chain plasmons will become degenerate with dipole resonance of noninteracting atoms. To gain insight into the formation of the end mode, we calculated the sodium chains with variable interatomic distances. Figure 5 shows the dipole strength of Na12 with d varied incrementally from 2.4 to 4.5 Å. The end and central modes exist in all cases. As d increases, both modes redshift in energy and the energy gap between them reduces from 0.56 eV at 2.4 Å to 0.17 eV at 4.5 Å, as expected. It is also clear that both the end and central modes are approaching the dipole resonance of the Na atom at 2.2 eV, where the arrow indicates. Such a trend is similar in chains of different lengths. It would be interesting to find out how the two modes evolve in energies and intensities as a function of d and how they merge into the single atomic resonance in the large d limit. Does this process occur continuously or as a dynamic Mott transition at some distance? Unfortunately, this is computationally beyond our reach due to the rapid increase in the number of grids with increasing d. Local-density approximation also becomes poor at large d, where nonlocal van der Waals interaction is expected to set in and dominate the interatomic interaction. Nevertheless, the trend in the evolution of the transverse excitations shown in Fig. 5 is in agreement with the qualitative analysis. The formation and strengths of the two transverse modes depend on the competition between the local atomic confinement and interatomic electron-electron interactions, although it is difficult to quantify their relative contributions in the present calculation.

To see whether these results are general to other atomic species, we have also done extensive calculations for different atomic chains. Figure 6(a) shows the excitation spectra of potassium chains with $d=3.72$ Å, the same interatomic distance used in Fig. 1 for sodium. Qualitatively, the K chains also show one L mode and two T modes, although their frequencies and strengths are slightly different from those of the Na chains. Detailed comparison indicates the following: (1) At the same length, the excitation energies of all three modes are smaller for the K chains, especially for the two T modes. This difference can be understood from the electronic structure. The 4s electron of K is more delocalized than the 3s electron of Na. The weaker binding of K atoms gives smaller highest occupied molecular orbital (HOMO)-lowest unoccupied molecular orbital (LUMO) gap and thus lower excitation energies. This explanation also applies for the energy differences in longer chains. (2) The strength of the end mode in K chains is smaller, about 2. It involves about one electron at each end compared with 2 in Na chains. The smaller strength of the end mode results from the weaker coupling between neighboring atoms. (3) Although the plas-

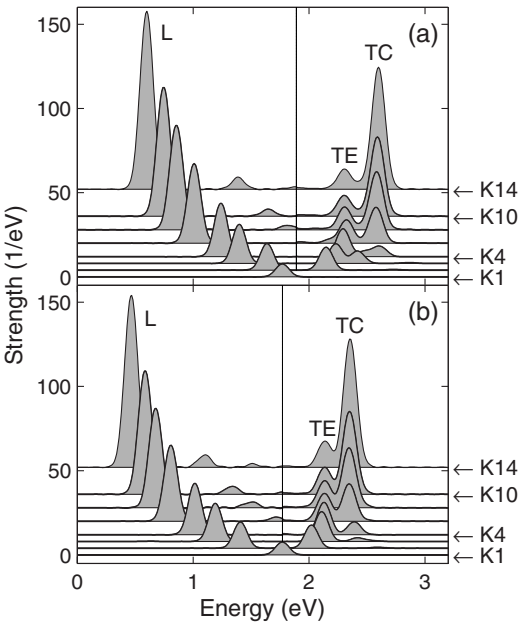

FIG. 6. The dipole response of linear potassium chains at two interatomic distances (a) d=3.72 Å and (b) d=4.54 Å excited in the longitudinal (left) and transverse (right) directions. The spectra correspond, counting from the bottom, to N=1, 2, 3, 4, 6, 8, 10, and 14.

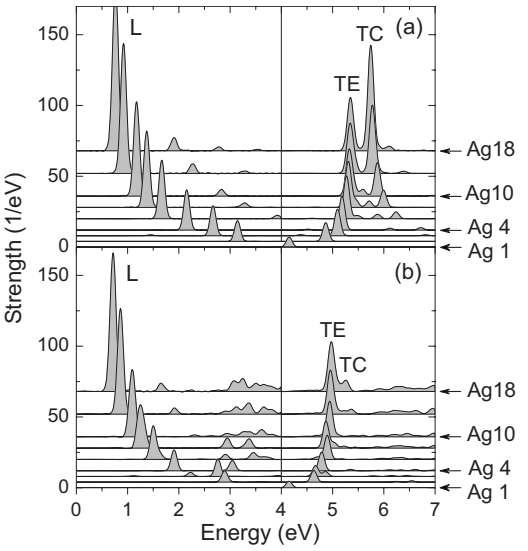

FIG. 7. The dipole response of linear silver chains calculated with (a) $5s^1$ and (b) $4d^{10}5s^1$ configurations of electrons in the valence. These spectra are obtained using an interatomic distance of 2.89 Å, corresponding to adsorbed silver chains on the NiAl(110) surface. The spectra in both panels have, counting from the bottom, N=1, 2, 3, 4, 6, 8, 10, 14, and 18.

mon energies are different between the two atomic chains, the energy splitting ΔE between the TC and TE modes is almost the same for both K and Na chains. For example, ΔE between TC and TE mode is 0.29 eV for K14, which is close to 0.28 eV for Na14. This seems to suggest that the energy gaps between the plasmon modes are primarily determined by the interatomic interactions and are insensitive to the local confinement within the atomic cores. This conclusion is further supported by excitation spectra calculated at d =4.54 Å, as shown in Fig. 6(b), which corresponds to the bond length of the K dimer. Increasing d leads to the same features as we observed on Na chains including the redshift in plasmon frequencies and the change in the strengths of the TE and TC modes. From the results of Na and K chains, we may conclude that most features obtained on Na chains are general characteristics of 1D plasmons in other chains.

B. Silver chains: Effect of *d* electrons

Noble metals such as silver have unusual optical properties in both bulk metals and clusters due to its d bands, which lie a few eV below the Fermi level. They can in principle participate in and damp the low-energy excitations associated with the free 5s electrons. Effect of d states on the optical absorption of clusters has been studied in the literature.[60,61,63,64] In bulk Ag, the plasmon energy, 3.8 eV,[65] is near the threshold 3.8–3.92 eV (Refs. 63 and 65) of d-p transitions. It was demonstrated that self-energy corrections to the electron energies by the GW scheme are essential to quantitatively reproduce the plasmon frequency of silver.[66] At surfaces, screening by the d electrons was found to reduce the energy of the surface plasmon of the jellium model from 6.5 to 3.7 eV,[64] while in small clusters, screening by the d electrons quenches the oscillator strengths by more than 50% compared to the free-electron-like metals.[61] Our interest here is to find out how the d states affect the plasmon resonances in the linear-chain geometry.

To that end, we performed two sets of time-dependent local-density approximation (TDLDA) calculations with pseudopotentials including and excluding the 4d electrons in the valence states, as given in Table I. Figure 7(a) shows the excitation spectra calculated with frozen d electrons. These excitation spectra are generally similar to those shown in Figs. 1 and 6 for free-electron metals with one L mode and two T resonances. The energies of the plasmons are slightly higher (for Ag18, ω_{L}=0.76 eV, ω_{TE}=5.35 eV, and ω_{TC} =5.74 eV) and the strength of the end mode is 6 (Ag), >4 (Na), or 2 (K). These differences can be qualitatively attributed to the competition between intra-atomic confinement and interatomic coupling. Large coupling, as is the case in Ag chains, favors a higher frequency and a stronger TE mode.

Figure 7(b) shows the spectra of silver chains calculated with $4d^{10}5s^1$ as valence electrons. At first, we benchmarked our results with previous calculations for Ag atoms and dimer in the literature. For monomer (the bottom curve), our calculation gives an excitation energy of 4.15 eV with an oscillator strength of 0.65, which are in good agreement with previous results: 4.13 eV and 0.66 (Ref. 60) vs 4.16 eV and 0.62.[61] They are also comparable to the experimental values of 3.74 eV and 0.7.[67,68] For the dimer, the two resonances at 2.89 and 4.63 eV are the L and T modes, respectively. These energies are slightly lower than those published in early calculations: 3.2 eV for the L mode and 4.75–4.9 eV for the T mode.[60,61] The minor difference (by up to 0.3 eV) was due to the larger bond length of 2.89 Å used in our case simulating

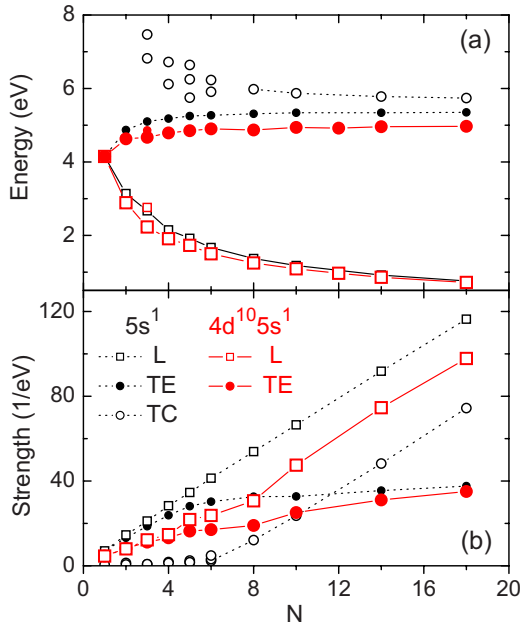

FIG. 8. (Color online) (a) The excitation energy and (b) dipole strength as functions of the number of atoms N for the resonance peaks shown in Fig. 7 with d electrons (red, gray) and without d electrons (black).

the adsorbed chains on NiAl(110),[51] in comparison with 2.61 Å (Ref. 60) and 2.57 Å (Ref. 61) used in earlier calculations. The good agreement among these data justifies the reliability of the pseudopotentials and our numerical calculations.

In longer chains, the longitudinal spectra in Fig. 7(b) are still similar to those in panel (a) without d electrons. Their excitation energies are almost the same, while the strengths are slightly reduced as shown more clearly in Fig. 8. Inclusion of the d states does not affect the longitudinal mode. This can be clearly seen in the induced densities as shown in Fig. 9 for the Ag12 chain. The longitudinal oscillations are dominated by 5s electrons. The interband (d-p) transitions are well above the longitudinal modes, so that d electrons do not participate in the longitudinal excitation. In real space,

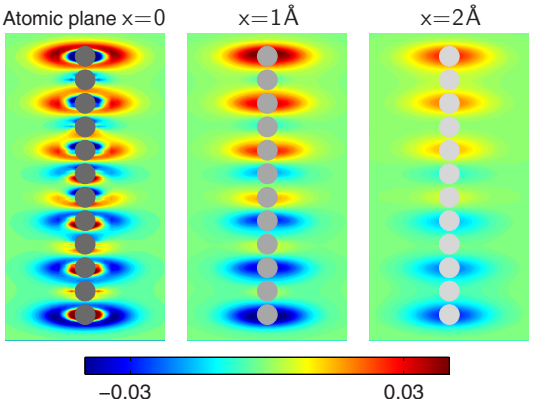

FIG. 9. (Color online) Fourier transforms of the induced densities for the Ag12 chain with d electrons at ω_L projected in the atomic plane $x=0$ and two other planes which offset by $x=1.0$ and 2.0 Å from the atomic plane.

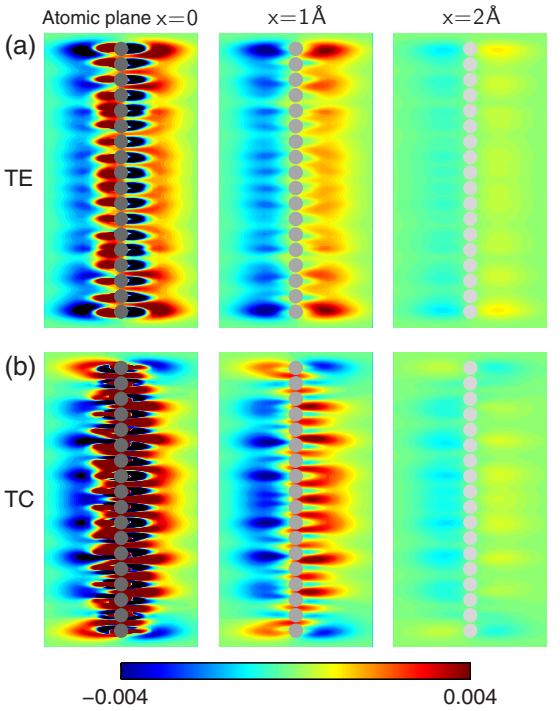

FIG. 10. (Color online) Fourier transforms of the induced densities of Ag18 at $x=0$, 1.0, 2.0 Å for the two transverse plasmon resonances of $\omega_{TE}=4.97$ eV (a) and $\omega_{TC}=5.26$ eV (b). See the text for discussion.

the longitudinal oscillations are much localized in the outer space of the atoms and do not overlap appreciably with the d electrons in the inner shell.

On the contrary, the transverse spectra in Fig. 7(b) look substantially different from those in panel (a). Only one peak (4.7–5.0 eV) is visible in short chains. A second broad band starts to develop in chains longer than ten atoms. In Ag18, a second mode appears as a shoulder at 5.26 eV beside the main peak. Charge density analysis shown in Fig. 10 of these modes shows that they are dominantly the end and central modes of the chain, although they are strongly mixed and damped by the d electrons. In planes ($x=1$ and 2 Å) which are offset from the atomic plane, the characteristics of the end and central modes can be seen more clearly. Figure 10 also provides a real-space picture of screening by the d electrons, which oscillate in the opposite direction as the free electrons and thus depolarize the electric field set up by the 5s electrons. This picture is very clear in the atomic plane ($x=0$ Å). Comparison of Figs. 9 and 10 suggests that screening in atomic chains is highly anisotropic due to the energetics of d-p transitions, which is only operative in the transverse excitations. In addition, more detailed inspection of the induced densities suggests that the stronger damping of the central mode may also be affected by the spatial distributions of the oscillations within the chains. For the TE mode, oscillations are localized on the end atoms which have effectively more free space without overlapping with that of d electrons. However, electrons of the TC mode penetrate the central region occupied by the d electrons, which may contribute to the stronger damping of the TC mode. The different behaviors of the plasmon resonances by the d bands dem-

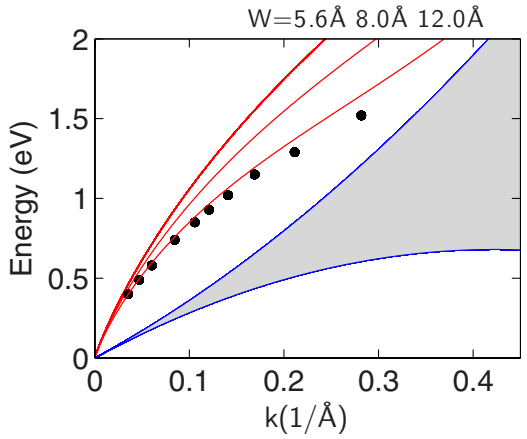

FIG. 11. (Color online) Plasmon dispersion relation of sodium chains (dots) corresponding to $N=3$, 4, 5, 6, 7, 8, 10, 14, 18, and 24. Lines are the plasmon dispersion of 1DEG with a linear density $n_1=1/d=0.269$ Å^{-1}. The only fitting parameter is the cylinder width W. Dispersion curves obtained with $W=5.6$, 8.0, and 12.0 Å are shown. Shaded area marks the continuum of electron-hole pair excitations.

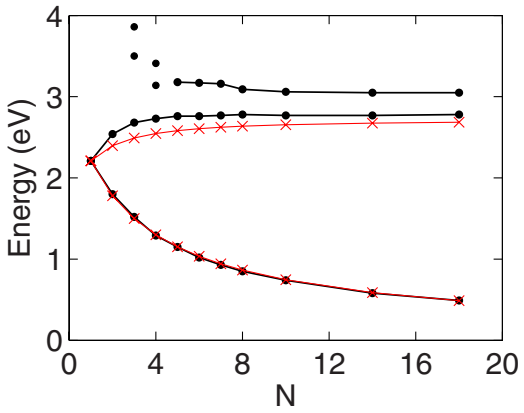

FIG. 12. (Color online) Comparison of plasmon energies of sodium chains calculated by TDLDA (dots) with the Mie frequencies of the ellipsoidal model (crosses).

onstrate once again that both geometry and electronic structure are essential to understand the plasmon resonances at atomic scales. Apart from the plasmon resonances, broad absorption bands show up in both the longitudinal spectra above 3 eV and transverse spectra above 5.5 eV. These broad bands are signatures of d-p transitions, which exist in both clusters and bulk metals. Figure 7 also indicates that the inclusion of d electrons gives a more reliable description of optical-absorption of silver chains.

C. Discussions

We now discuss a few aspects of 1D plasmon resonances in atomic chains and their general implications. These issues include, for example, (i) the dispersion of the plasmons in finite chains and its comparison with the 1DEG, (ii) a comparison between TDLDA and classical modeling of these resonances, and (iii) tunability of the plasmon resonances in the linear-chain geometry. These issues are generally interesting from the viewpoint of nanoplasmonics.

1. Energy dispersion of the longitudinal plasmon

The longitudinal resonance shows an energy that depends on the length of chains. The dipole character of the charge oscillations suggests that a standing wave with a half wavelength $\lambda/2=L=Nd$ can be associated with this resonance. The length dependence of the plasmon frequencies implies an energy dispersion, which shall approach to that of 1DEG in the long chain limit. It is interesting to find out how this dispersion develops in finite chains and how it compares with that of the 1DEG, which has been well studied in the literature.[50,69–71] Derivation of 1D band structure from the single-particle states of gold chains was studied in recent experiments.[47] Similar study has also been carried out for vibrational resonances in linear atomic chains.[72] In both cases, the dispersions of discrete resonance states of finite chains were found to agree with those of infinite chains. What is the case for collective plasmon excitation is yet to be seen.

Figure 11 shows the dispersion relation of the longitudinal resonances (dots) of sodium chains shown in Fig. 1(a). The red solid lines are the dispersion curves of a confined 1DEG model,[69,70] with parameters chosen to mimic the sodium chains.[73] The dispersion of longitudinal plasmon modes (dots) qualitatively follows those curves of the 1DEG model (solid lines). They are especially comparable in the long-wavelength limit, namely, for $N>4$ or $k<0.2$ Å^{-1}. A best fitting of dispersion can be obtained with $W=12$ Å, the confining radius of the 1DEG model. However this value is unphysically large compared with the atomic radius (3.6 Å) of the sodium atoms. With a smaller yet reasonable value, say $W=5.6$ Å, the energies of plasmon resonances are lower than those expected by the dispersion curve especially in short chains. This deviation reflects mainly the electron localization at the atomic sites, which becomes more prominent in short chains. In the long-chain limit, the energy of the chain plasmon decreases almost linearly with k and vanishes as k approaches zero. Both features are characteristic for plasmons in 1DEG. We would like to mention that similar dispersion was measured for Au atomic wires on Si surface.[50] In addition, the spectra of allowed single-particle excitations are also marked as the shaded area in Fig. 1(a). Unlike the three-dimensional (3D) electron gas, the plasmon energies of the chains are above $\omega_+(k)$ and never intersect with the electron-hole pair continuum at all wavelengths. The absence of Landau damping in 1D suggests that a long lifetime of 1D plasmons can be expected due to forbidden decay channels into electron-hole pairs.

2. Quantum vs classical comparison

While all the results were obtained by TDLDA, it is tempting to see whether these results are reproducible by any classical electrodynamic models. To answer this question, we simulate the atomic chains with a simple ellipsoid model, where analytical expressions for the Mie resonances are available. Figure 12 shows the plasmon frequencies (red cross) of the ellipsoidal model[74] with parameters chosen to

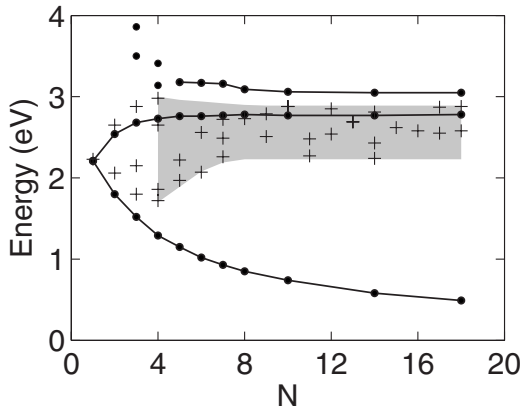

FIG. 13. Comparison of plasmon energies in sodium chains (dots) with those of sodium clusters (crosses and shaded area), which are obtained from Refs. 77–80.

mimic the sodium chains.[75] With $R \simeq 3.0$ Å and $\omega_p = 3.83$ eV,[76] we find a fairly good fitting to the longitudinal and central transverse modes as shown in Fig. 12. However, the ellipsoid model does not yield any end resonance, which lies above the transverse frequencies. The absence of the end mode may result from an artificial effect of the ellipsoid because the sharp ends of the ellipsoid may not support any end state. It may also indicate that end mode is purely a quantum-mechanical effect, which is not reproducible in a classical modeling. Further investigation of the end mode with other models such as, for example, the nanocylinder model is desirable to figure out this difference. Apart from disagreement in the end mode, it is still amazing to see that the longitudinal and central transverse resonances obtained by LR-TDLDA are so close to the Mie resonances of the ellipsoid model. The agreement is found for such a wide range of chain lengths with just a single and same set of parameters.

3. Tunability at atomic scale

Finally, we compare the plasmon frequencies of atomic chains with those of nanometer clusters to illustrate the atomic-scale tunability of 1D plasmon resonances of the chains. Such a comparison is of general interest for nanoplasmonic research and applications. The rapid development of nanoplasmonics is largely spurred by the possibility of engineering plasmon excitations with nanostructures. Future electronic and optical applications may ultimately involve plasmonic devices with atomic precision.

As one such comparison, Fig. 13 shows the plasmon energies of sodium chains (dots) and clusters (crosses and shaded area),[77–80] as a function of the number of atoms. The plasmon frequencies of the clusters are scattered due to multiple stable structures and nonspherical shapes at certain sizes. Despite the variations in frequencies, it is clear that the frequencies of the chain plasmons lie well beyond the energy range of their clusters. The transverse modes are generally larger while the longitudinal one lies well below the energy spectrum of the clusters. The frequencies of the clusters also show fewer variations with size. In fact, they are almost fixed by the size and polarization of the excitation. Linear atomic chains offer a wide spectrum of tunable plasmons ranging from ultraviolet to far-infrared regime. In addition to the tunable frequencies, different density responses in space of these resonances also open the possibility to control electron dynamics and its interaction with external excitations. Such tunability and control can be achieved down to atomic dimension.

IV. CONCLUDING REMARKS

We have carried out a systematic study of electronic excitations in linear atomic chains of both simple metals (Na and K) and noble metal (Ag) using time-dependent density-functional theory. Based on these calculations and results, the following conclusions can be drawn:

(1) Linear atomic chains generally sustain a longitudinal resonance, whose frequency depends on its length. The energy dispersion of the standing waves is comparable to that of the propagating plasmon waves in 1DEG.

(2) There are two transverse plasmon modes, the end and central modes, whose density responses are localized at the two ends and in the central region of the chains, respectively. These two modes resemble the surface and bulk plasmons of metal surfaces and thin films. The splitting of the transverse excitation into the end and central modes results from the competition between the interatomic coupling and the atomic confinement.

(3) The longitudinal excitation of silver chains is nearly unaffected by the *d* electrons, while the transverse plasmon modes are strongly suppressed and mixed by the *d* bands of silver atoms. This anisotropic screening is governed by the energetics of interband (*d*-*p*) transitions, which is only operative in the transverse excitations.

(4) The plasmon of the linear atomic chains is on one hand a model system for studying plasmonic properties at atomic scales. It also offers unique possibility to engineer tunable resonances in one dimension at atomic precision. The plasmons of the chains are very different from those of self-assembled clusters in both frequencies and in electron dynamics in real space.

These results provide physical insights into the plasmons at the conceptual level. In addition the first-principles calculation based on LR-TDLDA also compiled concise and first-hand data for the plasmons resonances of these linear chains. While these atom chains are available in modern laboratories, it is our belief that the results presented here will be directly comparable with experimental measurement in the near future.

ACKNOWLEDGMENTS

The authors thank Peter Nordlander for insightful discussions. This work was supported by the 100-Talent Program of the Chinese Academy of Sciences, the Institutional Grant Program of STINT, the Swedish Foundation for International Cooperation in Research and Higher Education, and the PhotoNano program of the Swedish Foundation for Strategic Research (SSF).

[1] S. Nie and S. R. Emory, Science **275**, 1102 (1997).
[2] H. X. Xu, E. J. Bjerneld, M. Käll, and L. Börjesson, Phys. Rev. Lett. **83**, 4357 (1999).
[3] Y. Sun and Y. Xia, Science **298**, 2176 (2002).
[4] C. Sönnichsen, T. Franzl, T. Wilk, G. von Plessen, J. Feldmann, O. Wilson, and P. Mulvaney, Phys. Rev. Lett. **88**, 077402 (2002).
[5] P.-A. Hervieux and J.-Y. Bigot, Phys. Rev. Lett. **92**, 197402 (2004).
[6] W. L. Barnes, A. Dereux, and T. W. Ebbesen, Nature (London) **424**, 824 (2003).
[7] J. B. Pendry, L. Martin-Moreno, and F. J. Garcia-Vidal, Science **305**, 847 (2004).
[8] J. Aizpurua, G. Hoffmann, S. P. Apell, and R. Berndt, Phys. Rev. Lett. **89**, 156803 (2002).
[9] J. Aizpurua, P. Hanarp, D. S. Sutherland, M. Käll, G. W. Bryant, and F. J. García de Abajo, Phys. Rev. Lett. **90**, 057401 (2003).
[10] J. Aizpurua, G. W. Bryant, L. J. Richter, F. J. García de Abajo, B. K. Kelley, and T. Mallouk, Phys. Rev. B **71**, 235420 (2005).
[11] I. Romero, J. Aizpurua, G. W. Bryant, and F. J. García de Abajo, Opt. Express **14**, 9988 (2006).
[12] J. Aizpurua and A. Rivacoba, Phys. Rev. B **78**, 035404 (2008).
[13] H. X. Xu and M. Käll, Phys. Rev. Lett. **89**, 246802 (2002).
[14] H. X. Xu, X. H. Wang, M. P. Persson, H. Q. Xu, M. Käll, and P. Johansson, Phys. Rev. Lett. **93**, 243002 (2004).
[15] E. Prodan, C. Radloff, N. J. Halas, and P. Nordlander, Science **302**, 419 (2003).
[16] E. Prodan and P. Nordlander, J. Chem. Phys. **120**, 5444 (2004).
[17] P. Nordlander, C. Oubre, E. Prodan, K. Li, and M. I. Stockman, Nano Lett. **4**, 899 (2004).
[18] P. Nordlander and E. Prodan, Nano Lett. **4**, 2209 (2004).
[19] F. Hao and P. Nordlander, Appl. Phys. Lett. **89**, 103101 (2006).
[20] F. Le, N. Z. Lwin, J. M. Steele, M. Käll, N. J. Halas, and P. Nordlander, Nano Lett. **5**, 2009 (2005).
[21] H. Wang, D. W. Brandl, P. Nordlander, and N. J. Halas, Acc. Chem. Res. **40**, 53 (2007).
[22] N. Fang, H. Lee, C. Sun, and X. Zhang, Science **308**, 534 (2005).
[23] A. T. Bell, Science **299**, 1688 (2003).
[24] L. R. Hirsch, R. J. Stafford, J. A. Bankson, S. R. Sershen, B. Rivera, R. E. Price, J. D. Hazle, N. J. Halas, and J. L. West, Proc. Natl. Acad. Sci. U.S.A. **100**, 13549 (2003).
[25] D. Pines, Rev. Mod. Phys. **28**, 184 (1956).
[26] A. Liebsch, *Electronic Excitations at Metal Surfaces* (Plenum, New York, 1997).
[27] P. J. Feibelman, Prog. Surf. Sci. **12**, 287 (1982).
[28] R. H. Ritchie, Phys. Rev. **106**, 874 (1957).
[29] H. Raether, *Surface Plasmons on Smooth and Rough Surfaces and on Gratings* (Springer-Verlag, Berlin, 1988).
[30] U. Kreibig and M. Vollmer, *Optical Properties of Metal Clusters* (Springer, Berlin, 1995).
[31] H. X. Xu, J. Aizpurua, M. Käll, and P. Apell, Phys. Rev. E **62**, 4318 (2000).
[32] Z. Yuan and S. W. Gao, Phys. Rev. B **73**, 155411 (2006).
[33] Z. Yuan and S. W. Gao, Surf. Sci. **602**, 460 (2008).
[34] C. Yannouleas and R. A. Broglia, Ann. Phys. (N.Y.) **217**, 105 (1992).
[35] G. Weick, R. A. Molina, D. Weinmann, and R. A. Jalabert, Phys. Rev. B **72**, 115410 (2005).
[36] G. Weick, G.-L. Ingold, R. A. Jalabert, and D. Weinmann, Phys. Rev. B **74**, 165421 (2006).
[37] T. M. Wallis, N. Nilius, and W. Ho, Phys. Rev. Lett. **89**, 236802 (2002).
[38] H. Ohnishi, Y. Kondo, and K. Takayanagi, Nature (London) **395**, 780 (1998).
[39] A. I. Yanson, G. R. Bollinger, H. E. van den Brom, N. Agraït, and J. M. van Ruitenbeek, Nature (London) **395**, 783 (1998).
[40] P. Gambardella, M. Blanc, H. Brune, K. Kuhnke, and K. Kern, Phys. Rev. B **61**, 2254 (2000).
[41] D. Sanchez-Portal, E. Artacho, J. Junquera, P. Ordejón, A. Garcia, and J. M. Soler, Phys. Rev. Lett. **83**, 3884 (1999).
[42] S. R. Bahn and K. W. Jacobsen, Phys. Rev. Lett. **87**, 266101 (2001).
[43] S. Fölsch, P. Hyldgaard, R. Koch, and K. H. Ploog, Phys. Rev. Lett. **92**, 056803 (2004).
[44] J. Lagoute, C. Nacci, and S. Fölsch, Phys. Rev. Lett. **98**, 146804 (2007).
[45] I. Barke, F. Zheng, T. K. Rügheimer, and F. J. Himpsel, Phys. Rev. Lett. **97**, 226405 (2006).
[46] J. N. Crain, M. D. Stiles, J. A. Stroscio, and D. T. Pierce, Phys. Rev. Lett. **96**, 156801 (2006).
[47] N. Nilius, T. M. Wallis, and W. Ho, Science **297**, 1853 (2002).
[48] J. N. Crain and D. T. Pierce, Science **307**, 703 (2005).
[49] P. Segovia, D. Purdie, M. Hengsberger, and Y. Baer, Nature (London) **402**, 504 (1999).
[50] T. Nagao, S. Yaginuma, T. Inaoka, and T. Sakurai, Phys. Rev. Lett. **97**, 116802 (2006).
[51] G. V. Nazin, X. H. Qiu, and W. Ho, Phys. Rev. Lett. **90**, 216110 (2003).
[52] D. C. Guhr, D. Rettinger, J. Boneberg, A. Erbe, P. Leiderer, and E. Scheer, Phys. Rev. Lett. **99**, 086801 (2007).
[53] S. W. Gao and Z. Yuan, Phys. Rev. B **72**, 121406(R) (2005).
[54] J. Yan, Z. Yuan, and S. W. Gao, Phys. Rev. Lett. **98**, 216602 (2007).
[55] M. A. L. Marques, A. Castro, G. F. Bertsch, and A. Rubio, Comput. Phys. Commun. **151**, 60 (2003).
[56] K. Yabana and G. F. Bertsch, Phys. Rev. B **54**, 4484 (1996).
[57] C. Jamorski, M. E. Casida, and D. R. Salahub, J. Chem. Phys. **104**, 5134 (1996).
[58] N. Troullier and J. L. Martins, Phys. Rev. B **43**, 1993 (1991).
[59] L. Kleinman and D. M. Bylander, Phys. Rev. Lett. **48**, 1425 (1982).
[60] K. Yabana and G. F. Bertsch, Phys. Rev. A **60**, 3809 (1999).
[61] J. C. Idrobo, S. Öğüt, and J. Jellinek, Phys. Rev. B **72**, 085445 (2005).
[62] *Table of Interatomic Distances and Configuration in Molecules and Ions*, edited by L. E. Sutton (Chemical Society, London, UK, 1965).
[63] M. A. Cazalilla, J. S. Dolado, A. Rubio, and P. M. Echenique, Phys. Rev. B **61**, 8033 (2000).
[64] A. Liebsch, Phys. Rev. Lett. **71**, 145 (1993).
[65] H. Ehrenreich and H. R. Philipp, Phys. Rev. **128**, 1622 (1962).
[66] A. Marini, R. Del Sole, and G. Onida, Phys. Rev. B **66**, 115101 (2002).
[67] C. E. Moore, *Atomic Energy Levels*, Natl. Bur. Stand. Circ. (U.S.) No. 467 (U.S. GPO, Washington, D.C., 1958), Vol. III; N. P. Penkin and I. Yu. Slavenas, Opt. Spektrosk. **15**, 9 (1963).
[68] S. Fedrigo, W. Harbich, and J. Buttet, Phys. Rev. B **47**, 10706 (1993).
[69] W. I. Friesen and B. Bergersen, J. Phys. C **13**, 6627 (1980).

[70] S. Das Sarma and E. H. Hwang, Phys. Rev. B **54**, 1936 (1996).
[71] A. R. Goñi, A. Pinczuk, J. S. Weiner, J. M. Calleja, B. S. Dennis, L. N. Pfeiffer, and K. W. West, Phys. Rev. Lett. **67**, 3298 (1991).
[72] K. Liu and S. W. Gao (unpublished).
[73] In the random-phase approximation (RPA), $\omega_p(k) = \sqrt{[A(k)\omega_+^2(k) - \omega_-^2(k)]/[A(k)-1]}$ with $A(k)=\exp[k\pi/v(k,W)]$. Here $v(k,W)$ is the Fourier transform of the Coulomb potential of 1DEG that is transversely confined within a cylinder of radius W (Refs. 69 and 70). $\omega_\pm(k)=|kk_F \pm \frac{1}{2}k^2|$ are the upper and lower bounds of single-electron excitation and k_F is the Fermi wave vector.
[74] L. D. Landau, E. M. Lifshitz, and L. P. Pitaevskii, *Electrodynamics of Continuous Media*, 2nd ed. (Pergamon, Oxford, 1984).
[75] The frequencies of the ellipsoid are determined by the poles of its polarizability $\alpha(\omega)=\frac{4\pi abc}{3}\frac{\epsilon(\omega)-\epsilon_m}{\epsilon_m+n_i[\epsilon(\omega)-\epsilon_m]}$. Here $\epsilon(\omega)$ and ϵ_m are the dielectric functions of the ellipsoid and the surrounding medium and a, b, c are the half axes of the ellipsoid. The form factor n_i, $i=a,b,c$ is calculated by $n_i = \frac{abc}{2}\int_0^\infty \frac{ds}{(s+i^2)\sqrt{(s+a^2)(s+b^2)(s+c^2)}}$. We used $\epsilon_m=1$ for the isolate chains and a Drude dielectric function $\epsilon(\omega)=1-\omega_p^2/\omega^2$ (Ref. 76). The geometry of the chains is given by $a=b=R$ and $c=R+(N-1)\times d/2$.
[76] N. V. Smith, Phys. Rev. **183**, 634 (1969).
[77] J. O. Joswig, L. O. Tunturivuori, and R. M. Nieminen, J. Chem. Phys. **128**, 014707 (2008).
[78] J. Borggreen, P. Chowdhury, N. Kebaïli, L. Lundsberg-Nielsen, K. Lützenkirchen, M. B. Nielsen, J. Pedersen, and H. D. Rasmussen, Phys. Rev. B **48**, 17507 (1993).
[79] K. Selby, V. Kresin, J. Masui, M. Vollmer, W. A. de Heer, A. Scheidemann, and W. D. Knight, Phys. Rev. B **43**, 4565 (1991).
[80] M. Schmidt and H. Haberland, Eur. Phys. J. D **6**, 109 (1999).